

X-ray Emission Spectroscopy at X-ray Free Electron Lasers: Limits to Observation of the Classical Spectroscopic Response for Electronic **Structure Analysis**

Scott C. Jensen,[†]

Brendan Sullivan,^{†,@}

Daniel A. Hartzler,^{†,\$}

Jose Meza Aguilar,^{‡,⊗}

Salah Awel,^{§,||} Saša Bajt, Shibom Basu, Richard Bean, Henry N. Chapman, S, II, V © Chelsie Conrad, Chapman, Chapman, Chapman, S, II, V © Chelsie Conrad, Chapman, Matthias Frank, Raimund Fromme, Jose M. Martin-Garcia, Thomas D. Grant, □,△ Michael Heymann,^{§,}

Mark S. Hunter, Gihan Ketawala, Richard A. Kirian, Juraj Knoska, Juraj Knoska, Sinda Ketawala, Sinda Ke Christopher Kupitz, Xuanxuan Li, Mengning Liang, Stella Lisova, Valerio Mariani, Victoria Mazalova, Marc Messerschmidt, Michael Moran, Garrett Nelson, Dominik Oberthür, Alex Schaffer, Raymond G. Sierra, Natalie Vaughn, Uwe Weierstall, 4,0 Max O. Wiedorn, J. P. Lourdu Xavier, Jay-How Yang, Oleksandr Yefanov, Nadia A. Zatsepin, Andrew Aquila, Petra Fromme, Sébastien Boutet, Gerald T. Seidler, and Yulia Pushkar*,†®

Supporting Information

Received: November 29, 2018 Accepted: December 19, 2018 Published: December 19, 2018

Department of Physics and Astronomy, Purdue University, West Lafayette, Indiana 47907, United States

[‡]Biodesign Institute, Center for Applied Structural Discovery, Arizona State University, 85287-5301, United States

[§]Center for Free-Electron Laser Science, Deutsches Elektronen-Synchrotron, D-22607 Hamburg, Germany

The Hamburg Center for Ultrafast Imaging, Universität Hamburg, 22761 Hamburg, Germany

¹Deutsches Elektronen-Synchrotron, D-22607 Hamburg, Germany

^{*}Paul Sherrer Institut (PSI), 5232 Villigen, Switzerland

[¶]European XFEL GmbH, D-22671 Hamburg, Germany

^VDepartment of Physics, Universität Hamburg, 22761 Hamburg, Germany

Lawrence Livermore National Laboratory, Livermore, California 94550, United States

Hauptman-Woodward Institute, Department of Structural Biology, Jacobs School of Medicine and Biomedical Sciences, SUNY University at Buffalo, Buffalo, New York 14203, United States

[△]BioXFEL Science and Technology Center, Buffalo, New York 14203, United States

Max Planck Institute of Biochemistry, 82152 Planegg, Germany

^OSLAC National Accelerator Laboratory, Menlo Park, California 94025, United States

Department of Physics, Arizona State University, Tempe, Arizona 85287-7401, United States

[◆]Department of Physics, University of Wisconsin—Milwaukee, Milwaukee, Wisconsin 53201, United States

Beijing Computational Science Research Center, Beijing 100193, China

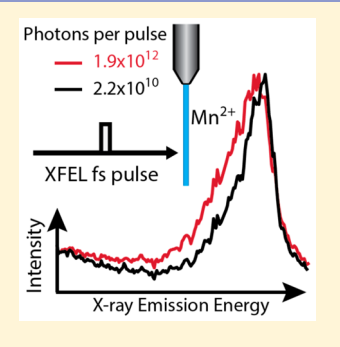
Department of Biochemistry, University of California Davis, Davis, California 95616, United States

Max-Planck Institute for the Structure and Dynamics of Matter, D-22761 Hamburg, Germany

School of Molecular Sciences, Arizona State University, Tempe, Arizona 85287-1604, United States

Department of Physics, University of Washington, Seattle, Washington 98195-1560, United States

ABSTRACT: X-ray free electron lasers (XFELs) provide ultrashort intense X-ray pulses suitable to probe electron dynamics but can also induce a multitude of nonlinear excitation processes. These affect spectroscopic measurements and interpretation, particularly for upcoming brighter XFELs. Here we identify and discuss the limits to observing classical spectroscopy, where only one photon is absorbed per atom for a Mn²⁺ in a light element (O, C, H) environment. X-ray emission spectroscopy (XES) with different incident photon energies, pulse intensities, and pulse durations is presented. A rate equation model based on sequential ionization and relaxation events is used to calculate populations of multiply ionized states during a single pulse and to explain the observed X-ray induced spectral lines shifts. This model provides easy estimation of spectral shifts, which is essential for experimental designs at XFELs and illustrates that shorter X-ray pulses will not overcome sequential ionization but can reduce electron cascade effects.



With the development of X-ray free electron laser (XFEL) sources, there has been a paradigm shift in X-ray scattering and spectroscopy studies for physics, chemistry, biology, and material sciences. With shorter (10–100 fs), more energetic (~10¹² photons) pulses, scientists can now study the atomic structure of nanocrystals, ¹ small molecules, ² and envision obtaining atomic resolution images for large single particles. ³ Ultrashort pulses also enable X-ray spectroscopic studies of chemical reactions with subpicosecond resolution, ^{4–6} revealing fundamental transitions such as electron transfer and bond formation dynamics. ⁷

While the X-ray community has been invigorated by these new opportunities, further research is required to understand the fundamental changes in the electronic structure of atoms due to the interaction with ultrashort (<100 fs), intense X-ray pulses. In this regime, nonlinear effects become significant as they distort electron energy levels and create new excited states. ^{12,13} While there is limited understanding of how these modified electronic configurations can influence X-ray diffraction results or the single particle scattering analysis planned at future sources, X-ray spectroscopy can clearly be affected by the formation of electronic states beyond the one electron excitations typically analyzed at synchrotron sources, Figure 1.

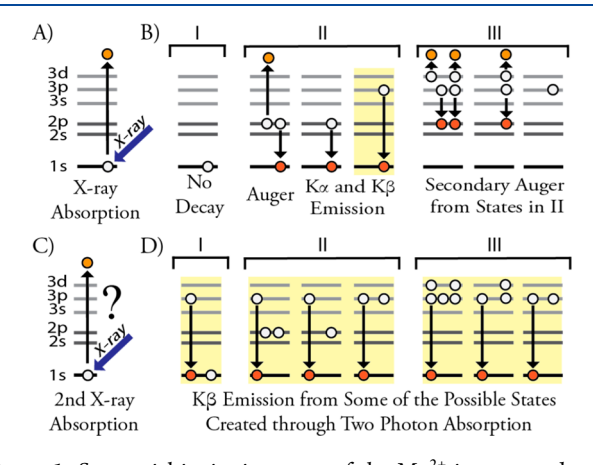


Figure 1. Sequential ionization steps of the $\mathrm{Mn^{2^+}}$ ion exposed to an intense X-ray pulse. Highlighted in yellow are the recorded emission processes. (A) X-ray absorption creating a hole in the 1s orbital. (B) Possible electronic states obtained on different time scales: (I) no decay, (II) 1s hole filled, and (III) 2s and 2p holes filled. (C) Second 1s hole created. (D) Subsequent decay (only $\mathrm{K}\beta$ shown) in the presence of various electronic configurations shown in part B, which alter spectral positions. Note that Auger processes can create a variety of different states in II and III that are not shown.

Understanding these effects will aid the development of the proper experimental protocols and interpretation of electronic structure measurements depending on time scales and intensities of the utilized X-ray pulses.

Here ions of a 3d transition metal (Mn²⁺) in a lighter element (O, C, H) environment are used as a model system for 3d transition metals in general and for the biologically relevant $\rm Mn_4Ca$ cluster inside photosystem $\rm II^{14}$ in particular. Radiationinduced damage to Mn centers in photosystem II at a synchrotron source is caused by chemical interaction of oxidized Mn ions with reactive species such as photoelectrons and OH* radicals. 15 As these damaging mechanisms require time for chemical redox processes to take place, they can be largely outrun at femtosecond XFEL sources. 16-19 Despite this, there are still two sources of electronic changes that need to be considered during a single XFEL pulse: sequential X-ray absorption by a single atom, Figure 1, and secondary ionizations caused by released photoelectrons and Auger electrons.²⁰⁻²³ While these effects have been observed at XFELs previously, it remains unclear to what extent multiple ionization effects may impact interpretation of spectroscopic or crystallographic data.

Here effects of the intensity and duration of the XEFL pulse on the electronic structure of Mn ions were analyzed by X-ray emission spectroscopy (XES), Figure 2. The $K\beta$ emission

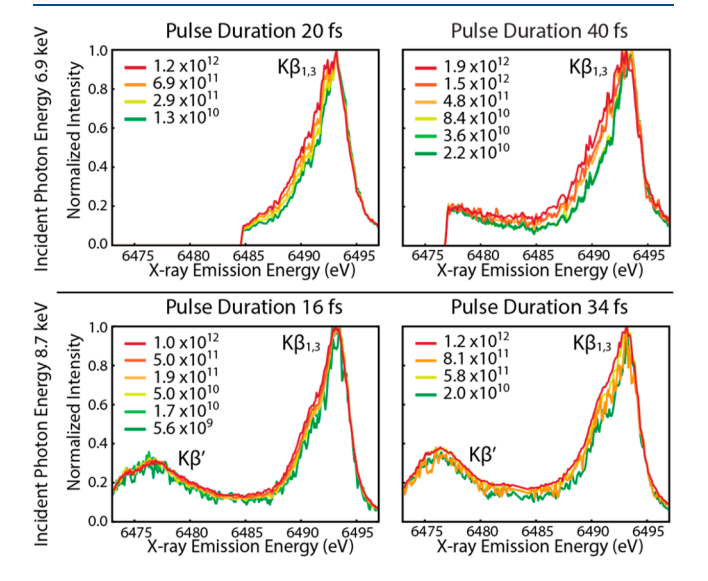


Figure 2. Mn K β spectra recorded with varying photons per pulse colored green to red for increasing values. Different excitation energies (top, 6.9 keV; bottom, 8.7 keV), pulse intensity and pulse durations are also shown. The K β' region is only available in the lower graphs due to the differences in spectrometer positioning inside the vacuum chamber. Broadening of the low energy side of the K $\beta_{1,3}$ line with increased pulse intensity is visible.

The Journal of Physical Chemistry Letters

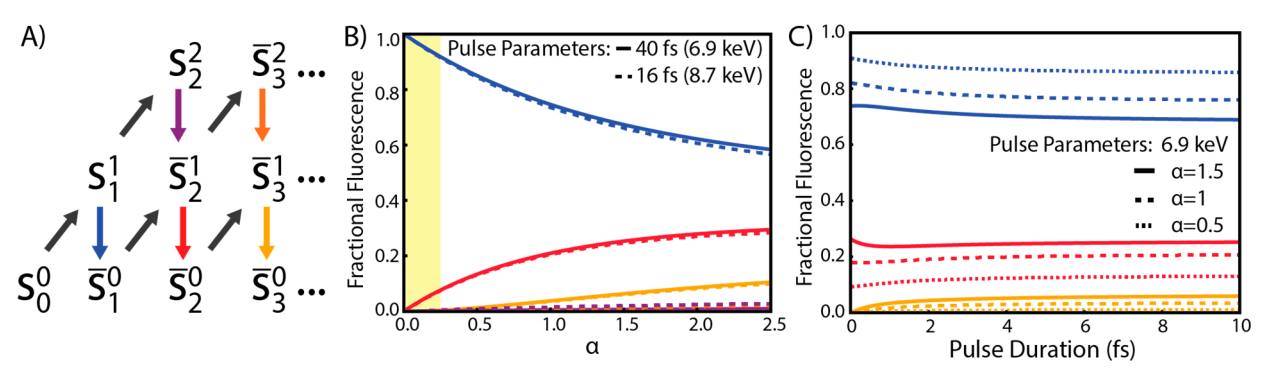


Figure 3. (A) Rate equation model with each state, S, labeled by the number of 1s holes (superscript) and total 1s absorption events (subscript) with the bar above indicating that there are multiple electronic configurations in this state. Arrows going up indicate 1s absorption, and arrows down are electronic relaxation filling a 1s hole. Colors are referenced to differentiate $K\beta$ emission from different states with blue representing classical emission. (B) Contributions to the total $K\beta$ fluorescence based on decay from five different states with colors matching those in (A) with an approximately linear regime highlighted in yellow. (C) Contributions to the total recorded $K\beta$ fluorescence as a function of pulse duration.

spectrum is a result of the 3p to 1s transitions after a 1s core hole is created, Figure 1B–II (last diagram to the right). The exchange interaction between the newly created 3p hole and the valence electrons on the Mn 3d level leads to two spectral features ($K\beta'$ and $K\beta_{1,3}$) with splitting sensitive to the oxidation state and spin state of Mn. ^{24–27} XES in conjunction with XFEL pulses is used to probe fast dynamics, dilute samples and new electronic states with applications in surface chemistry, ⁴ solvent shell dynamics ²⁸ and electron transfer. ²⁹ However, all these applications require collection of the classical (or singly ionized) spectra for proper interpretation.

Here XES is used to monitor emission from Mn²⁺ ions absorbing one or more X-ray photons. Multiple ionizations are shown to induce changes to the spectra of 3d transition metal ions (Mn) in a low-Z(O, C, H) environment which is similar to protein complexes such as photosystem II. The Mn K β XES spectra recorded from Mn²⁺ ions (jetted 1 M MnCl₂ in H₂O or ethanol; see Supporting Information Methods) are shown in Figure 2. Each panel represents one of four different XFEL pulse configurations recorded: 20 and 40 fs pulse durations using 6.9 keV incident photon energy as well as 16 and 34 fs at 8.7 keV incident photon energy. For each pulse configuration, the Mn $K\beta_{1,3}$ peak shifts to lower energy with the increase of the pulse intensity. The onset of electronic structure changes in the Mn ion due to the interaction with the XFEL pulse creates a different XES spectra from the low flux regime, where only one X-ray photon is absorbed per atom, as Figures 1 and 2 illustrate.

To address the spectral shape change induced by sequential ionization, we used theoretical modeling of electronic states obtained during a single XFEL pulse using rate equations 20,21,30 shown schematically in Figure 3A. The initial population starts in the ground state, S_0^0 , as Mn^{2+} with no 1s holes. During X-ray exposure, the Mn atom will populate the different states labeled as S_k^j where j is the current number of 1s holes in the atom (maximum of two) and k shows the total number of 1s absorption events the atom has undergone. Any atom in a specific state can advance forward through ionization of a 1s electron if one is available. The rate for this process A^j , or absorption rate, is written as

$$A^j = \Phi \sigma^j$$

where Φ is the photon flux density, or photons per area per time and σ^j is the atomic photoelectric cross section for the 1s orbital with j holes in the same orbital. The atom can also go to a lower j state, downward in Figure 3A, by filling a 1s hole through Auger

decay or fluorescence. These effects combined have a decay rate, D_k^j where j and k represent the state from which the decay occurs. The decay rate, the probability of $K\beta$ emission, and the 1s cross sections were calculated using XATOM, which has been described in detail elsewhere. The beam profile was assumed to be Gaussian, making Φ radially dependent. The photon flux density was approximated stepwise to capture this dependence in the model as described in the Supporting Information Methods section.

With this model the fractional population of Mn centers that have absorbed at least one X-ray photon, i.e., no longer in the S_0^0 state, is

$$P_{\rm abs} = 1 - e^{-A^j t}$$

where t is the pulse duration. Approximating the exponent, A^jt , as the parameter α defined via basic experimental parameters and using the full width half-maximum (FWHM) of the X-ray spot size, the following is obtained

$$\alpha \equiv \sigma^0 \frac{0.5(\text{photons per pulse})}{\text{area}}$$

where σ^0 is the photoelectric cross section for the filled 1s orbital of a single atom, "0.5(photons per pulse)" is the number of photons in the FWHM profile of the X-ray beam, and the "area" is the X-ray spot size within the FWHM profile. Rewriting the absorbing fractional population, the following is obtained,

$$P_{\rm abs} \cong 1 - e^{-\alpha}$$

The parameter α is introduced here as it encapsulates most of the pulse duration, photon density, and spot size behavior in the model allowing for an easy comparison of data sets obtained with different X-ray parameters.

Figure 3B shows, as a function of α , the proportion of the $K\beta$ emission that results from different fluorescent decays (depicted by the same colors as in Figure 3A). From this plot the onset of sequential ionization effects can be clearly seen. The percent of the total $K\beta$ emission which corresponds to classical emission (blue) can be estimated for small values of α (the highlighted region) to be

classical fluorescence
$$\cong 100\% - 34\alpha$$
 where $\alpha \le 0.25$

This is a useful measure for understanding the convolution of emitting states when XES measurements are planned at an XFEL.

The rate equation model can also be used to predict the X-ray induced shifts in the first moment of the $K\beta_{1,3}$ peak by treating each electron hole as one oxidation state shift (see Supporting Information Methods). The first moment of each data set shown in Figure 2 is calculated as $FM = \frac{\sum E_i I_i}{\sum I_i}$ where E_i is the emission energy and I_i is the intensity of the spectrum using the energy between 6485 and 6495 eV with 0.1 eV bins. The change in first moment, typically used as an estimate for the oxidation state²⁵ or localized spin density changes,³³ is shown for each data set in Figure 4 to indicate the

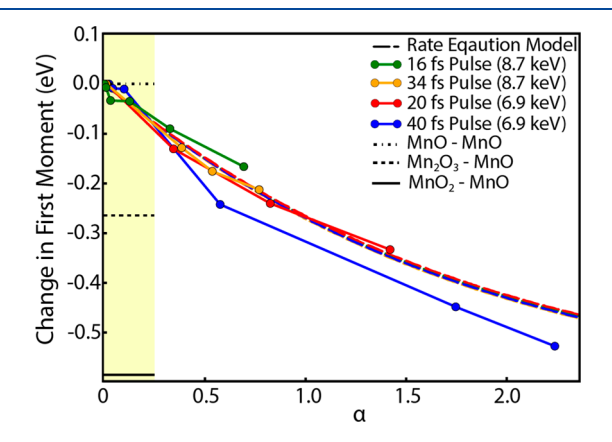


Figure 4. First moment dependence on α for four data sets. For each data set α is increasing with an increase of number of photons per pulse. The rate equation predictions for the four data sets are represented by dashed lines with colors matching the respective data set; however, all of the models overlap due to nearly identical dependence on the parameter α . The region with approximately linear dependence of the FM on α is highlighted. The three horizontal bars in the highlighted region show the difference between the FM values of Mn³⁺ and Mn⁴⁺ oxides from the reference Mn²⁺ oxide to indicate typical FM shifts between different oxidation states of Mn ions.

sample's electronic structure changes with increasing pulse intensity.

The model predictions shown in Figure 4 appear to be in good agreement with the FM shifts in the data. We do note, however, that while the model predicts a nearly identical α dependence for each set of parameters, the data appear to have additional dependence on the pulse duration and incident photon energy. These effects are likely a result of additional ionization processes caused by Auger and photoelectrons. The increasing cross section of light elements at lower energy and more secondary ionizations during longer pulse durations will likely result in larger spectral changes and FM shifts. Additionally, the data sets with different incident photon energies were taken during different beamtimes and small changes in the FWHM of the beam may also be responsible for some of the FM shift between the two photon energies used.

To predict the FM shift in XES data for Mn ions and other high spin 3d ions, we refer to the linear regime in Figure 4. Here the first moment shift in the linear regime, highlighted in Figures 3B and 4, can be estimated as

$$FM_{shift} \cong -0.3\alpha$$
 when $\alpha \leq 0.25$

This simple analysis is useful in estimating tolerable photon densities based on XFEL parameters for experimental setups. This is important for some systems, such as photosystem II, where FM shifts of interest may be as small as ~ 0.02 eV in the S₂ to S₃ state transition. ^{25,34} For detection of such small spectral

changes it is clearly best to be removed from equivalent X-ray induced shifts estimated here, especially when additional effects from the electron cascade may be involved.

It is important to note that $\alpha \sim 0.5$ was used in an earlier XFEL based study recording X-ray emission spectra of MnCl₂. The uncertainty in alignment of classical emission from a synchrotron and data collected at an XFEL was ~ 0.05 eV which should not have precluded the detection of an X-ray induced shift predicted by the model presented here. As no detectable shift was observed, the same X-ray beam parameters were used for XES analysis of PSII. While the source of discrepancy is currently unknown, we do emphasize that predictions provided here should be carefully considered when XFEL experiments are planned.

As XFEL sources move toward shorter and shorter pulses, achieving subfemtosecond durations, it is important to take into account the potential and limitation of outrunning X-ray induced electronic changes that affect measurements. For the electron cascade, it seems to be clear that shorter pulses will lead to fewer electron-electron interactions.³⁷ From a sequential ionization standpoint, the picture is more complicated. As shorter pulse durations with the same photon densities are used, a larger population of the atoms will reach the empty 1s state. Atoms in this state will decay twice to fully repopulate the 1s orbital. Since the emission from atoms in the 1s⁰ state is likely to be significantly shifted relative to the 1s1 single hole state emission,³⁸ the former emission is not expected to contribute to the final spectral shape and is not shown in Figure 3C. However, after the 1s⁰ decay a subsequent emission from the 1s¹ state can occur and is expected to have spectral lines that overlap with the classical emission spectra. The second decay will have a higher probability of occurring in the presence of another low lying hole in the n = 2 shell given the short amount of time after dual core hole decay and single core hole decay, Figure 1B-II. This will result in different spectral line positions compared to longer pulses used here that give more time for further relaxation of the electronic structure such that holes are in the n = 3 level, Figure 1B-III. Nevertheless, the ratio of classical emission spectra to spectra from sequential ionization remains essentially unchanged as shorter X-ray pulses are used, as is shown in Figure 3C.

Since sequential ionization is dependent on α , lowering the number of photons, increasing the beam spot size, and increasing the incident photon energy all reduce the effect of sequential ionization. Out of the methods for reducing FM shifts, only increasing the X-ray spot size will not have a proportional reduction in the X-ray emission signal. Judging by our data, higher incident photon energies have the advantage over beam attenuation in that they will also reduce effects from photoelectrons of low Z elements by lowering their cross section. Shorter pulses will also lead to fewer electron interactions within the sample during the duration of the pulse.

While the potential for outrunning the electron cascade is important, emission spectra will still have similar FM shifts from sequential ionization, Figure 3C. Stimulated emission is one possible mechanism for increasing the emission intensity; however, the increased decay rate through stimulated emission may cause more sequential ionization events by refilling the 1s more rapidly, allowing more ionizations. This 1s repopulation process is likely the cause of photon intensity dependent spectral line shifts for Mn atoms undergoing stimulated emission observed previously. Ultrashort pulses can also lead to dual core hole ionization, which creates hypersatellite emission lines, or emission lines from the 1s⁰ state, that do not overlap spectroscopically with single core hole emission spectra. This allows X-ray pulses that

create dual ionization but are much shorter than the decay rate of these states to capture unaltered atomic hypersatellites, though various holes in surrounding atoms will likely impact the spectra of metal complexes as well as direct photoionization of electrons in orbitals other than the 1s. While some work has been done with hypersatellites experimentally, 40 more groundwork will be required before hypersatellites can be validated as a widely applicable spectroscopic technique for XES.

Here we present a rate equation model that quantifies the percentages of recorded $K\beta$ X-ray emission from atoms that have undergone a single or multiple sequential ionization events. Excellent agreement between the theoretical model and experimental observations has been demonstrated. Using the rate equation model discussed herein, we provide a simple method to estimate the percent of classical fluorescence vs fluorescence originated from sequentially ionized states and the associated FM shift. Deviation from the sequential ionization model is attributed to electron cascade. Methods of avoiding effects from these two sources are also discussed. Additionally, we note that shorter pulses do not overcome spectral changes that arise from sequential ionization and photon densities will have to be considered carefully in future facilities as more intense pulses become routinely available.

ASSOCIATED CONTENT

S Supporting Information

The Supporting Information is available free of charge on the ACS Publications website at DOI: 10.1021/acs.jpclett.8b03595.

Methods and procedures, emission from different states as a function of pulse duration (Figure S1), and X-ray emission data, photoelectric cross sections, and decay pathways and yields (Tables S1–S3) (PDF)

AUTHOR INFORMATION

Corresponding Author

*E-mail: ypushkar@purdue.edu.

ORCID ®

Scott C. Jensen: 0000-0002-8446-4800 Brendan Sullivan: 0000-0001-5271-8821 Henry N. Chapman: 0000-0002-4655-1743 Gerald T. Seidler: 0000-0001-6738-7930 Yulia Pushkar: 0000-0001-7949-6472

Present Addresses

^(a)Neutron Scattering Division, Oak Ridge National Laboratory, Oak Ridge, TN 37830, USA.

^{\$}Battelle, 626 Cochrans Mill Road, Pittsburgh, PA 15263, USA. [⊗]European XFEL GmbH, D-22671 Hamburg, Germany.

ONational Cancer Institute, National Institutes of Health, Bethesda, Maryland 20892, United States.

*Biodesign Institute, Arizona State University, Tempe, Arizona 85287-7401, United States.

⁷School of Molecular Sciences, Arizona State University, Tempe, Arizona 85287-1604, United States.

Notes

The authors declare no competing financial interest.

ACKNOWLEDGMENTS

We acknowledge Marius Schmidt, Abbas Ourmazd, Ahmad Hosseinizadeh, and Peter Schwander for help in data collection during the two beamtimes. The experiments were carried out during beamtimes LJ49 and LL23 (PI Petra Fromme) at

beamline CXI at the Linac Coherent Light Source, a national user facility operated by Stanford University on behalf of the US Department of Energy (DOE), Office of Basic Energy Sciences (OBES). Use of the Linac Coherent Light Source (LCLS), SLAC National Accelerator Laboratory, is supported by the U.S. Department of Energy, Office of Science, Office of Basic Energy Sciences under Contract No. DE-AC02-76SF00515. Parts of the sample delivery system used at LCLS for this research was funded by the NIH grant P41GM103393, formerly P41RR001209. This work was supported by the following agencies: the National Science Foundation, Division of Chemistry CHE-1350909 (Y.P.) the National Institutes of Health (award 1R01GM095583) (P.F.). This work was supported by the National Science Foundation (NSF)-Science and Technology Center (STC) "BioXFEL" through award STC-1231306, by funds from the National Institutes of Health grant R01 GM095583 as well as funds from the Biodesign Center for Applied Structural Discovery at Arizona State University. This work is also supported by the AXSIS project funded by the European Research Council under the European Union Seventh Framework Program (FP/2007-2013)/ERC Grant Agreement no. 609920. G.T.S. acknowledges support by the Joint Plasma Physics Program of the National Science Foundation and the Department of Energy under Grant No. DESC0016251. This work was performed, in part, under the auspices of the U.S. Department of Energy by Lawrence Livermore National Laboratory under Contract DE-AC52-07NA27344. M.F. was supported by the NIH grant 1R01GM117342-01.

REFERENCES

- (1) Chapman, H. N.; Fromme, P.; Barty, A.; White, T. A.; Kirian, R. A.; Aquila, A.; Hunter, M. S.; Schulz, J.; DePonte, D. P.; Weierstall, U.; et al. Femtosecond X-ray protein nanocrystallography. *Nature* **2011**, 470, 73–77.
- (2) Küpper, J.; Stern, S.; Holmegaard, L.; Filsinger, F.; Rouzée, A.; Rudenko, A.; Johnsson, P.; Martin, A. V.; Adolph, M.; Aquila, A.; et al. X-ray diffraction from isolated and strongly aligned gas-phase molecules with a free-electron laser. *Phys. Rev. Lett.* **2014**, *112*, 083002.
- (3) Aquila, A.; Barty, A.; Bostedt, C.; Boutet, S.; Carini, G.; DePonte, D.; Drell, P.; Doniach, S.; Downing, K. H.; Earnest, T.; et al. The linac coherent light source single particle imaging road map. *Struct. Dyn.* **2015**, *2*, 041701–041701.
- (4) Katayama, T.; Anniyev, T.; Beye, M.; Coffee, R.; Dell'Angela, M.; Föhlisch, A.; Gladh, J.; Kaya, S.; Krupin, O.; Nilsson, A.; et al. Ultrafast soft X-ray emission spectroscopy of surface adsorbates using an X-ray free electron laser. *J. Electron Spectrosc. Relat. Phenom.* **2013**, 187, 9–14.
- (5) Lemke, H. T.; Bressler, C.; Chen, L. X.; Fritz, D. M.; Gaffney, K. J.; Galler, A.; Gawelda, W.; Haldrup, K.; Hartsock, R. W.; Ihee, H.; et al. Femtosecond X-ray absorption spectroscopy at a hard X-ray free electron laser: application to spin crossover dynamics. *J. Phys. Chem. A* **2013**, *117*, 735–740.
- (6) McFarland, B. K.; Farrell, J. P.; Miyabe, S.; Tarantelli, F.; Aguilar, A.; Berrah, N.; Bostedt, C.; Bozek, J. D.; Bucksbaum, P. H.; Castagna, J. C.; et al. Ultrafast X-ray Auger probing of photoexcited molecular dynamics. *Nat. Commun.* **2014**, *5*, 4235.
- (7) Öström, H.; Öberg, H.; Xin, H.; LaRue, J.; Beye, M.; Dell'Angela, M.; Gladh, J.; Ng, M. L.; Sellberg, J. A.; Kaya, S.; et al. Probing the transition state region in catalytic CO oxidation on Ru. *Science* **2015**, 347, 978–982.
- (8) Doumy, G.; Roedig, C.; Son, S. K.; Blaga, C. I.; DiChiara, A. D.; Santra, R.; Berrah, N.; Bostedt, C.; Bozek, J. D.; Bucksbaum, P. H.; et al. Nonlinear Atomic Response to Intense Ultrashort X Rays. *Phys. Rev. Lett.* **2011**, *106*, 083002.
- (9) Larsson, M.; Salén, P.; van der Meulen, P.; Schmidt, H. T.; Thomas, R. D.; Feifel, R.; Piancastelli, M. N.; Fang, L.; Murphy, B. F.; Osipov, T.; et al. Double core-hole formation in small molecules at the

- LCLS free electron laser. J. Phys. B: At., Mol. Opt. Phys. 2013, 46, 164030-164030.
- (10) Tamasaku, K.; Shigemasa, E.; Inubushi, Y.; Katayama, T.; Sawada, K.; Yumoto, H.; Ohashi, H.; Mimura, H.; Yabashi, M.; Yamauchi, K.; et al. X-ray two-photon absorption competing against single and sequential multiphoton processes. *Nat. Photonics* **2014**, *8*, 313–316.
- (11) Fukuzawa, H.; Son, S. K.; Motomura, K.; Mondal, S.; Nagaya, K.; Wada, S.; Liu, X. J.; Feifel, R.; Tachibana, T.; Ito, Y.; et al. Deep innershell multiphoton ionization by intense x-ray free-electron laser pulses. *Phys. Rev. Lett.* **2013**, *110*, 173005.
- (12) Kanter, E. P.; Krässig, B.; Li, Y.; March, A. M.; Ho, P.; Rohringer, N.; Santra, R.; Southworth, S. H.; DiMauro, L. F.; Doumy, G.; et al. Unveiling and Driving Hidden Resonances with High-Fluence, High-Intensity X-Ray Pulses. *Phys. Rev. Lett.* **2011**, *107*, 233001.
- (13) Ho, P. J.; Bostedt, C.; Schorb, S.; Young, L. Theoretical tracking of resonance-enhanced multiple ionization pathways in X-ray free-electron laser pulses. *Phys. Rev. Lett.* **2014**, *113*, 253001.
- (14) Vinyard, D.; Brudvig, G.; Johnson, M.; Martinez, T. Progress Toward a Molecular Mechanism of Water Oxidation in Photosystem II. *Annu. Rev. Phys. Chem.* **2017**, *68*, 101–116.
- (15) Davis, K. M.; Kosheleva, I.; Henning, R. W.; Seidler, G. T.; Pushkar, Y. Kinetic modeling of the X-ray-induced damage to a metalloprotein. *J. Phys. Chem. B* **2013**, *117*, 9161–9169.
- (16) Suga, M.; Akita, F.; Hirata, K.; Ueno, G.; Murakami, H.; Nakajima, Y.; Shimizu, T.; Yamashita, K.; Yamamoto, M.; Ago, H.; et al. Native structure of photosystem II at 1.95 Å resolution viewed by femtosecond X-ray pulses. *Nature* **2015**, *517*, 99–103.
- (17) Young, I. D.; Ibrahim, M.; Chatterjee, R.; Gul, S.; Fuller, F. D.; Koroidov, S.; Brewster, A. S.; Tran, R.; Alonso-Mori, R.; Kroll, T.; et al. Structure of photosystem II and substrate binding at room temperature. *Nature* **2016**, *540*, 453–457.
- (18) Suga, M.; Akita, F.; Sugahara, M.; Kubo, M.; Nakajima, Y.; Nakane, T.; Yamashita, K.; Umena, Y.; Nakabayashi, M.; Yamane, T.; et al. Light-induced structural changes and the site of O = O bond formation in PSII caught by XFEL. *Nature* **2017**, *543*, 131–135.
- (19) Kupitz, C.; Basu, S.; Grotjohann, I.; Fromme, R.; Zatsepin, N. A.; Rendek, K. N.; Hunter, M. S.; Shoeman, R. L.; White, T. A.; Wang, D.; et al. Serial time-resolved crystallography of photosystem II using a femtosecond X-ray laser. *Nature* **2014**, *513*, 261–265.
- (20) Young, L.; Kanter, E. P.; Krassig, B.; Li, Y.; March, A. M.; Pratt, S. T.; Santra, R.; Southworth, S. H.; Rohringer, N.; Dimauro, L. F.; et al. Femtosecond electronic response of atoms to ultra-intense X-rays. *Nature* **2010**, *466*, 56–61.
- (21) Rohringer, N.; Santra, R. X-ray nonlinear optical processes using a self-amplified spontaneous emission free-electron laser. *Phys. Rev. A: At., Mol., Opt. Phys.* **2007**, *76*, 033416.
- (22) Cryan, J. P.; Glownia, J. M.; Andreasson, J.; Belkacem, A.; Berrah, N.; Blaga, C. I.; Bostedt, C.; Bozek, J.; Buth, C.; Dimauro, L. F.; et al. Auger electron angular distribution of double core-hole states in the molecular reference frame. *Phys. Rev. Lett.* **2010**, *105*, 083004.
- (23) Jurek, Z.; Son, S. K.; Ziaja, B.; Santra, R. XMDYN and XATOM: versatile simulation tools for quantitative modeling of X-ray free-electron laser induced dynamics of matter. *J. Appl. Crystallogr.* **2016**, *49*, 1048–1056.
- (24) Glatzel, P.; Bergmann, U. High resolution 1s core hole X-ray spectroscopy in 3d transition metal complexes electronic and structural information. *Coord. Chem. Rev.* **2005**, 249, 65–95.
- (25) Messinger, J.; Robblee, J. H.; Bergmann, U.; Fernandez, C.; Glatzel, P.; Visser, H.; Cinco, R. M.; McFarlane, K. L.; Bellacchio, E.; Pizarro, S. A.; et al. Absence of Mn-Centered Oxidation in the S₂ to S₃ Transition: Implications for the Mechanism of Photosynthetic Water Oxidation. *J. Am. Chem. Soc.* **2001**, *123*, 7804–7820.
- (26) Tsutsumi, K.; Nakamori, H.; Ichikawa, K. X-ray manganese K.beta. emission spectra of manganese oxides and manganates. *Phys. Rev. B: Condens. Matter Mater. Phys.* **1976**, *13*, 929–933.
- (27) Peng, G.; deGroot, F. M. F.; Hämäläinen, K.; Moore, J. A.; Wang, X.; Grush, M. M.; Hastings, J. B.; Siddons, D. P.; Armstrong, W. H.; Mullins, O. C.; et al. High-Resolution Manganese X-ray Fluorescence

- Spectroscopy. Oxidation-State and Spin-State Sensitivity. J. Am. Chem. Soc. 1994, 116, 2914–2920.
- (28) Haldrup, K.; Gawelda, W.; Abela, R.; Alonso-Mori, R.; Bergmann, U.; Bordage, A.; Cammarata, M.; Canton, S. E.; Dohn, A. O.; van Driel, T. B.; et al. Observing Solvation Dynamics with Simultaneous Femtosecond X-ray Emission Spectroscopy and X-ray Scattering. *J. Phys. Chem. B* **2016**, *120*, 1158–1168.
- (29) Canton, S. E.; Kjær, K. S.; Vankó, G.; van Driel, T. B.; Adachi, S.; Bordage, A.; Bressler, C.; Chabera, P.; Christensen, M.; Dohn, A. O.; et al. Visualizing the non-equilibrium dynamics of photoinduced intramolecular electron transfer with femtosecond X-ray pulses. *Nat. Commun.* **2015**, *6*, 6359–6359.
- (30) Makris, M. G.; Lambropoulos, P.; Mihelic, A. Theory of Multiphoton Multielectron Ionization of Xenon under Strong 93-eV Radiation. *Phys. Rev. Lett.* **2009**, *102*, 033002.
- (31) Son, S.-K.; Young, L.; Santra, R. Impact of hollow-atom formation on coherent x-ray scattering at high intensity. *Phys. Rev. A: At., Mol., Opt. Phys.* **2011**, 83, 033402.
- (32) Jurek, Z.; Santra, R.; Son, S.-K.; Ziaja, B. XRAYPAC A Software Package for Modeling X-Ray-Induced Dynamics of Matter, 1.01; CFEL, DESY, 2017.
- (33) Jensen, S. C.; Davis, K. M.; Sullivan, B.; Hartzler, D. A.; Seidler, G. T.; Casa, D. M.; Kasman, E.; Colmer, H. E.; Massie, A. A.; Jackson, T. A.; et al. X-ray Emission Spectroscopy of Biomimetic Mn Coordination Complexes. J. Phys. Chem. Lett. 2017, 8, 2584–2589.
- (34) Davis, K. M.; Sullivan, B. T.; Palenik, M. C.; Yan, L. F.; Purohit, V.; Robison, G.; Kosheleva, I.; Henning, R. W.; Seidler, G. T.; Pushkar, Y. Rapid Evolution of the Photosystem II Electronic Structure during Water Splitting. *Phys. Rev. X* **2018**, *8*, 041014.
- (35) Alonso-Mori, R.; Kern, J.; Gildea, R. J.; Sokaras, D.; Weng, T.-C.; Lassalle-Kaiser, B.; Tran, R.; Hattne, J.; Laksmono, H.; Hellmich, J.; et al. Energy-dispersive X-ray emission spectroscopy using an X-ray free-electron laser in a shot-by-shot mode. *Proc. Natl. Acad. Sci. U. S. A.* **2012**, *109*, 19103–19107.
- (36) Kern, J.; Alonso-Mori, R.; Tran, R.; Hattne, J.; Gildea, R. J.; Echols, N.; Glöckner, C.; Hellmich, J.; Laksmono, H.; Sierra, R. G.; et al. Simultaneous femtosecond X-ray spectroscopy and diffraction of photosystem II at room temperature. *Science* **2013**, *340*, 491–495.
- (37) Chapman, H. N.; Caleman, C.; Timneanu, N. Diffraction before destruction. *Philos. Trans. R. Soc., B* **2014**, *369*, 20130313.
- (38) Rosmej, F. B.; Dachicourt, R.; Deschaud, B.; Khaghani, D.; Dozières, M.; Šmíd, M.; Renner, O. Exotic x-ray emission from dense plasmas. J. Phys. B: At., Mol. Opt. Phys. 2015, 48, 224005.
- (39) Kroll, T.; Weninger, C.; Alonso-Mori, R.; Sokaras, D.; Zhu, D.; Mercadier, L.; Majety, V.; Marinelli, A.; Lutman, A.; Guetg, M.; et al. Stimulated X-Ray Emission Spectroscopy in Transition Metal Complexes. *Phys. Rev. Lett.* **2018**, *120*, 133203.
- (40) Berrah, N.; Fang, L.; Murphy, B.; Osipov, T.; Ueda, K.; Kukk, E.; Feifel, R.; van der Meulen, P.; Salen, P.; Schmidt, H. T.; et al. Double-core-hole spectroscopy for chemical analysis with an intense X-ray femtosecond laser. *Proc. Natl. Acad. Sci. U. S. A.* **2011**, *108*, 16912–16915.